Latest LHCb results from the pA data

Liang Zhong
Tsinghua University, Beijing, China
E-mail: liang.zhong@cern.ch

Abstract. The J/ψ production cross-sections in proton-nucleus collisions at $\sqrt{s} = 5$ TeV are measured using the LHCb detector. A sizable suppression is observed in pA forward collisions, while only a slight suppression is seen in pA backward collisions. The nuclear attenuation factor $R_{p\mathrm{A}}$ and the forward-backward production ratio r_{FB} are determined.

1. Introduction

The suppression of heavy quarkonia production is a probe to explore quark-gluon plasma (QGP). However, the suppression can also be caused by cold nuclear matter effects (CNM). In proton-nucleus (pA) collisions QGP cannot be created, while CNM can still occur. Hence pA collision can separate the contribution of QGP and CNM. This provides important inputs to heavy ion collisions, where QGP and CNM are entangled.

The LHCb detector [1] is a single-arm forward spectrometer covering the pseudorapidity range $2 < \eta < 5$. The detector includes a high precision tracking system consisting of a silicon-strip vertex detector (VELO) surrounding the pp interaction region, a large-area silicon-strip detector located upstream of a dipole magnet with a bending power of about 4 Tm, and three stations of silicon-strip detectors and straw drift tubes placed downstream. The combined tracking system has a momentum resolution that varies from 0.4% at 5 GeV/c to 0.6% at 100 GeV/c, and an impact parameter resolution of 20 μm for tracks with high transverse momentum (p_{T}). Charged hadrons are identified using two ring-imaging Cherenkov detectors. Photon, electron and hadron candidates are identified by a calorimeter system consisting of scintillating-pad and preshower detectors, an electromagnetic calorimeter and a hadronic calorimeter. Muons are identified by a system composed of alternating layers of iron and multiwire proportional chambers. The trigger [2] consists of a hardware stage, based on information from the calorimeter and muon systems, followed by a software stage which applies a full event reconstruction.

The LHC carries out pA collisions by colliding a proton beam with an energy of 4 TeV and a lead beam with an energy of 1.58 TeV per nucleon. This corresponds to a proton-nucleon centre-of-mass energy of $\sqrt{s} = 5$ TeV. The instantaneous luminosity in pA collisions is $5 \times 10^{27}\mathrm{cm}^{-2}\mathrm{s}^{-1}$, which is five orders of magnitude below the nominal luminosity in pp collisions. The directions of the proton and lead beams are swapped between the data taking periods. The configuration with the direction of travel of the protons from the VELO to the muon system (the muon system to the VELO) is referred to as producing pA forward (backward) collisions. Positive rapidity (y) in the proton-nucleon centre-of-mass system (CM) is always defined to be the direction of the proton beam. The rapidity coverage in the CM is shifted due to the asymmetric beam

energy, which results in a rapidity coverage of $1.5 < y < 4.0$ for pA forward collisions and $-5.0 < y < -2.5$ for pA backward collisions.

The dataset used in this analysis was collected during the proton-nucleus run in early 2013. The samples used for this analysis correspond to integrated luminosities of 0.75 nb^{-1} for forward collisions and 0.30 nb^{-1} for backward collisions. Simulated samples based on pp collisions are used to estimate acceptance and reconstruction efficiencies. In case of significant differences between simulated sample and data, the simulated samples are re-weighted to match the data.

2. J/ψ production measurement

The strategy of the J/ψ production cross-section measurement follows the previous measurements at LHCb [3, 4, 5]. There are three sources of J/ψ mesons in proton-nucleus collisions: direct production in the collisions, feed-down from higher charmonium states, and the decay of b hadrons. Those produced by the first two sources are referred to as prompt J/ψ mesons, and those from the third as J/ψ mesons from b hadrons (abbreviated as "J/ψ from b" in the following). The prompt J/ψ mesons and J/ψ from b carry different information of CNM, therefore their cross-sections should be measured separately.

The double differential cross-section is defined as

$$\frac{\mathrm{d}^2\sigma}{\mathrm{dp_T dy}} = \frac{N(J/\psi \to \mu^+\mu^-)}{\varepsilon L \mathcal{B}(J/\psi \to \mu^+\mu^-)\Delta p_\mathrm{T} \Delta y}, \tag{1}$$

where $N(J/\psi \to \mu^+\mu^-)$ is the observed number of J/ψ, ε the efficiency, L the integrated luminosity, $\mathcal{B}(J/\psi \to \mu^+\mu^-)$ the branching ratio of $J/\psi \to \mu^+\mu^-$ [6], Δp_T the p_T bin width and Δy the y bin width.

The J/ψ candidates are reconstructed from dimuon final states. Muons with high p_T in the final states are selected, and good fit qualities of tracks and vertices are required. An unbinned maximum likelihood fit is performed to extract the number of signal candidates. The signal peak is fitted with a Crystal Ball function [7], and the background with an exponential function.

The prompt J/ψ mesons decay at the primary vertex (PV), while the J/ψ from b hadrons decay at a sizable distance from the PV because of the large lifetimes of b hadrons. The pseudo-proper-time t_z is employed to distinguish prompt J/ψ mesons and J/ψ from b. It is defined as

$$t_z \equiv \frac{(z_{J/\psi} - z_\mathrm{PV}) M_{J/\psi}}{p_z}, \tag{2}$$

where $z_{J/\psi}$ is the z position of the J/ψ decay vertex, z_PV that of the primary vertex refitted after removing the two muon tracks of the J/ψ candidate, p_z the momentum projection of the J/ψ candidate along the beam axis, and $M_{J/\psi}$ the invariant mass of the J/ψ candidate.

The t_z distribution of prompt J/ψ mesons is described by a δ-function convolved with a double-Gaussian function, and that of J/ψ from b by an exponential function convolved with a double Gaussian function. For the background, the t_z distribution is modelled by an empirical function based on the shape of the t_z distribution observed in the J/ψ mass sidebands.

The cross-sections of the prompt J/ψ mesons and J/ψ from b are obtained by a simultaneous fit to the invariant mass and the t_z distribution of the J/ψ candidates. The projections of the fit are shown in Fig. 1.

The measured double differential cross-sections for prompt J/ψ mesons and J/ψ from b in pA forward collisions as a function of p_T and y, assuming no J/ψ polarisation, are shown in Fig. 2. The single differential cross-sections for prompt J/ψ mesons and J/ψ from b in pA forward and pA backward collisions as a function of p_T and y are displayed in Fig. 3 and 4, respectively.

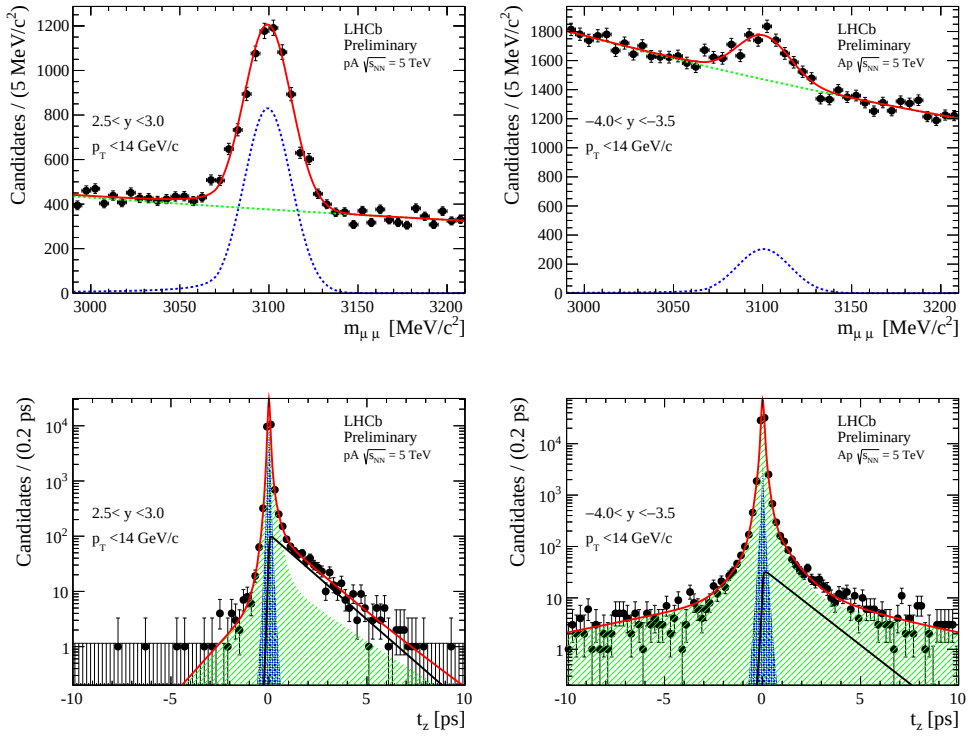

Figure 1. Fit to (top) the invariant mass and (bottom) pseudo-proper-time of the J/ψ candidates for (left) pA forward and (right) pA backward collisions.

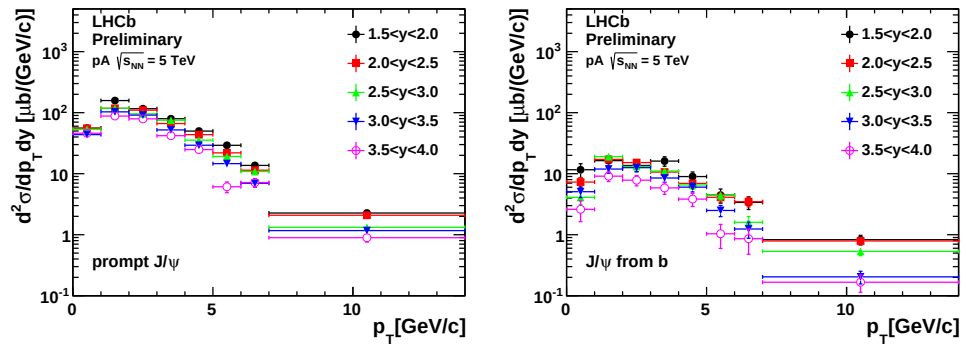

(a) (b)

Figure 2. Double differential cross-section of (left) prompt J/ψ mesons and (right) J/ψ from b as functions of $p_{\rm T}$ in bins of y in pA forward collisions.

The integrated cross-sections for prompt J/ψ mesons in pA forward and backward collisions and in pp collisions are compared in the common rapidity region, $2.5 < |y| < 4.0$. The J/ψ cross-section in pp collisions at $\sqrt{s} = 5$ TeV is determined to be $4.78 \pm 0.23 \pm 0.15$ μb by interpolating the cross-sections at 2.76, 7, and 8 TeV [3, 4, 5]. After integration over the common rapidity region and the full $p_{\rm T}$ range, the cross-sections are scaled by a factor of $1/A$, where A is 208 for pA collisions, and 1 for pp collisions. The scaled results are shown in Fig. 5. Clear suppression is observed in forward collisions, while only a mild suppression is observed in backward collisions.

Quarkonia production cross-sections in pA collisions are expected to be sensitive to CNM.

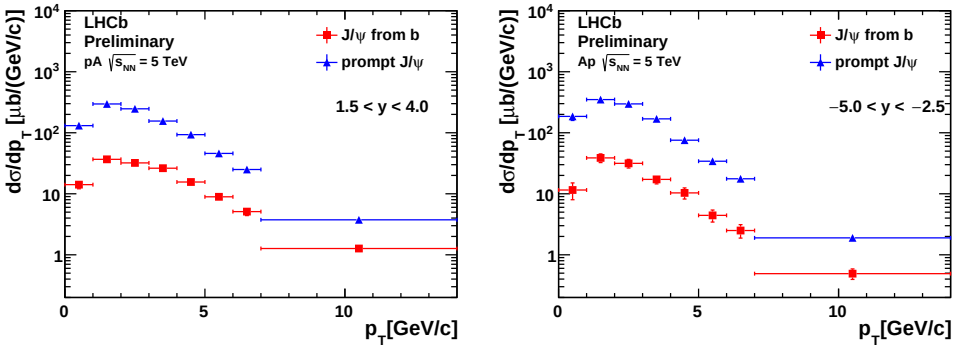

(a) (b)

Figure 3. Single differential cross-section of (red) prompt J/ψ mesons and (blue) J/ψ from b for (left) pA and (right) pA backward collisions as a function of $p_{\rm T}$.

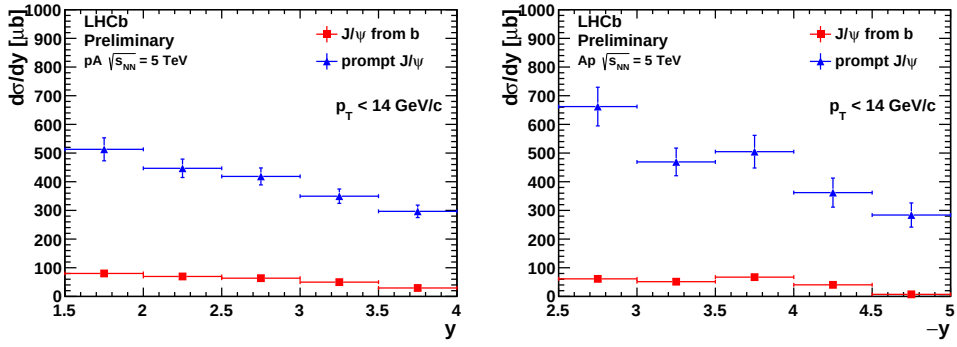

(a) (b)

Figure 4. Single differential cross-section of (red) prompt J/ψ mesons and (blue) J/ψ from b for (left) pA and (right) pA backward collisions as a function of y.

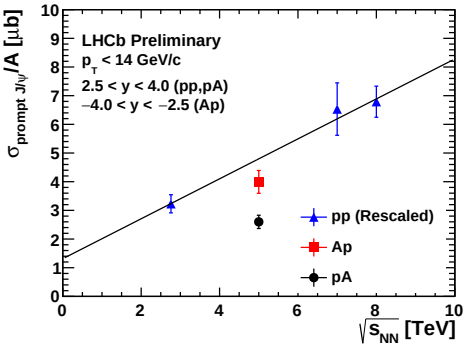

Figure 5. The cross-sections for prompt J/ψ mesons scaled by a factor of $1/A$ in the common rapidity range of $2.5 < |y| < 4.0$ for pp, pA forward, and pA backward collisions. The blue triangles are the cross-sections at 2.76, 7 and 8 TeV in the same kinematic region, the black line is a linear fit to the blue triangles, the red dot is the cross-section in pA backward collisions, and the black dot is the cross-section in pA forward collisions.

Comparisons of J/ψ production cross-sections in pA and pp collisions can shed light on these effects. The nuclear attenuation factor

$$R_{p\rm A}(|y|,\sqrt{s_{\rm NN}}) = \frac{1}{A}\frac{\frac{{\rm d}\sigma_{\rm pA}}{{\rm d}y}(|y|,\sqrt{s_{\rm NN}})}{\frac{{\rm d}\sigma_{\rm pp}}{{\rm d}y}(|y|,\sqrt{s_{\rm NN}})} \tag{3}$$

is evaluated as a function of y and compared to theoretical models [8] in Fig. 6(a). Within the

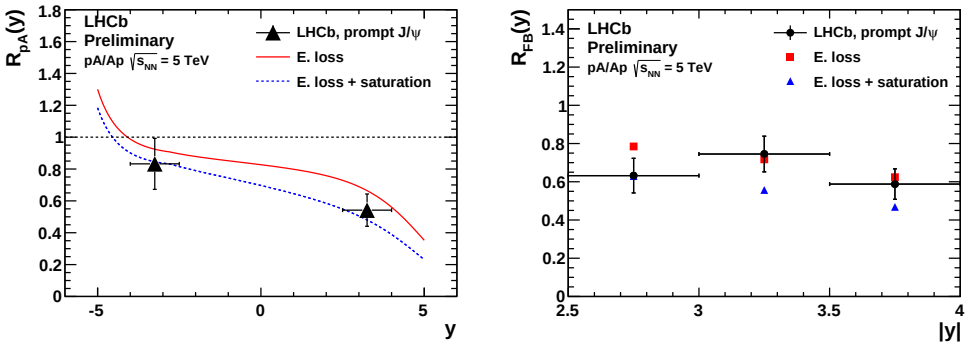

(a) (b)

Figure 6. Comparisons of (a) the attenuation factor $R_{p\mathrm{A}}$ and (b) the forward-backward production ratio r_{FB} between data and theory. The black triangles (diamonds) are the LHCb results, the red solid line (squares) are the theoretical prediction based on parton energy loss effects, and the blue dotted line (triangles) are a model with additional saturation effects in the left (right) plot.

current precision the data do not distinguish between the models with or without saturation effects.

The production of J/ψ mesons is found to have a forward-backward asymmetry [9, 10]. This is quantified by the forward-backward production ratio, $r_{\mathrm{FB}}(y) = R_{p\mathrm{A}}(y)/R_{\mathrm{A}p}(y)$. With the current precision, the data do not discriminate between the models from Ref. [8] with and without saturation effects.

3. Conclusion

The differential cross-sections of J/ψ mesons are measured with the LHCb detector using data collected in pA collisions at $\sqrt{s_{\mathrm{NN}}} = 5$ TeV [11]. Clear suppression is observed in forward collisions, while only a mild suppression is seen in backward collisions. The nuclear attenuation factor $R_{p\mathrm{A}}$ and the forward-backward production ratio r_{FB} are determined, and the preliminary results are consistent with theoretical predictions and the results of ALICE [12].

References

[1] Alves Jr A A *et al.* 2008 *JINST* **3** S08005
[2] Aaij R *et al.* 2013 *JINST* **8** P04022 (*Preprint* hep-ex/1211.3055)
[3] Aaij R *et al.* (LHCb Collaboration) 2011 *Eur. Phys. J. C* **71** 1645 (*Preprint* hep-ex/1103.0423)
[4] Aaij R *et al.* (LHCb Collaboration) 2013 *J. High Energy Phys.* **1302** 041 (*Preprint* hep-ex/1212.1045)
[5] Aaij R *et al.* (LHCb Collaboration) 2013 *J. High Energy Phys.* **1306** 064 (*Preprint* hep-ex/1304.6977)
[6] Beringer J *et al.* 2012 *Phys. Rev.* D **86** 010001
[7] Skwarnicki T 1986 *A study of the radiative cascade transitions between the Upsilon-Prime and Upsilon resonances* Ph.D. thesis
[8] Arleo F and Peigne S 2013 *J. High Energy Phys.* **1303** 122 (*Preprint* hep-ph/1212.0434)
[9] Leitch M *et al.* (FNAL E866/NuSea Collaboration) 2000 *Phys. Rev. Lett.* **84** 3256–3260 (*Preprint* nucl-ex/9909007)
[10] Adare A *et al.* (PHENIX Collaboration) 2011 *Phys.Rev.Lett.* **107** 142301 (*Preprint* nucl-ex/1010.1246)
[11] Aaij R *et al.* (LHCb Collaboration) 2013 (*Preprint* nucl-ex/1308.6729)
[12] Abelev B B *et al.* (ALICE Collaboration) 2013 (*Preprint* nucl-ex/1308.6726)